Free-Standing Nanomembranes Based on Selective CVD Deposition of Functional Poly-*p*-xylylenes

Florence Bally-Le Gall,[†,‡] Christian Friedmann,[†] Lars Heinke,[†] Hassan Arslan,[†] Carlos Azucena,[†] Alexander Welle,[†,§] Aftin M. Ross,[†,∥] Christof Wöll,[*,†] and Jörg Lahann[*,†,∥]

[†]Institute of Functional Interfaces, Karlsruhe Institute of Technology, Eggenstein-Leopoldshafen, 76344, Germany, [‡]Institute of Materials Science of Mulhouse (IS2M, UMR 7361), University of Upper Alsace (UHA), Mulhouse, 68093, France, [§]Karlsruhe Nano Micro Facility (KNMF), Karlsruhe Institute of Technology, Eggenstein-Leopoldshafen, 76344, Germany, and [∥]Biointerfaces Institute, Department of Macromolecular Science and Engineering and Department of Chemical Engineering, University of Michigan, Ann Arbor, Michigan 48109, United States

ABSTRACT The precise engineering of ultrathin nanofilms with variable functionality remains an unmet challenge in nanotechnology. We report a strategy for generating free-standing nanomembranes based on the selective chemical vapor deposition polymerization of functional [2.2]paracyclophanes on micropatterned self-assembled monolayers of alkanethiolates on gold. This fabrication strategy can yield microstructured nanofilms that are between 2 and 5 nm thick. Subsequent release from the substrate results in free-standing nanoscale membranes with controlled pore size and geometry. The process allows for modification of important functional parameters, such as ultrasmall membrane thickness, membrane pore geometry, and chemical functionality.

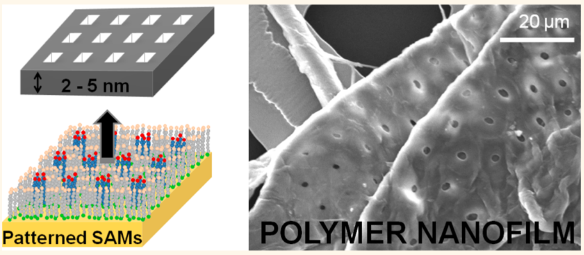

KEYWORDS: chemical vapor deposition · microstructured nanofilm · self-assembled monolayer · nanocarpet · nanomembrane

In the field of nano- and biotechnologies, the synthesis of chemically functionalized nanosheets and nanomembranes remains a continuous technological challenge. Ultrathin, two-dimensional nanomaterials typically cover areas of square micrometers to centimeters but have a thickness of only tens of nanometers or even less. Several techniques have already been reported for the fabrication of such nanosheets,[1,2] including nanosheets based on graphene[3,4] or polymer.[5,6] Similarly, functional polymer nanomembranes have been produced by electron-induced cross-linking of aromatic monolayer films.[7,8] While extremely thin membranes were obtained using this approach, the choices for chemical functionalization of the nanosheets remain somewhat limited. Higher functional diversity can be achieved when layer-by-layer (LBL) deposition of polyelectrolytes[9] and inorganic filler materials[10,11] are used. However, this method is restricted to the use of polyionic compounds. In some specialized examples, nanosheets have also been prepared by self-assembly of triblock copolymers,[12] via Langmuir–Blodgett transfer,[13] or by spin-coating of a polymer solution.[14,15] The aforementioned techniques usually result in nanosheets that are tens of nanometers thick, which may be prohibitive for some applications.

Supported functional nanofilms of only a few nanometers have previously been prepared by chemical vapor deposition polymerization.[16,17] The vapor-based polymerization of [2.2]paracyclophanes using the Gorham route is among the most studied processes yielding poly-*p*-xylylene films.[18] A wide variety of functional groups[19] can be introduced by this method, effectively decoupling surface and bulk chemistry. This robust, solvent-free process enables the fabrication of pinhole-free polymer films. Their thickness can be easily tuned by controlling the amount of precursor used for CVD polymerization.[20] The resulting reactive coatings can be patterned by different methods, in which the patterning occurs either in the form of a postmodification

* Address correspondence to lahann@umich.edu, christof.woell@kit.edu.

Received for review October 9, 2014 and accepted February 3, 2015.

10.1021/nn505761x

reaction or during the CVD process. While patterning methods such as microcontact printing,[21] photopatterning,[22] or dip-pen nanolithography[23] create covalent bonds and demand wet-chemical conditions, direct patterning during the CVD process has also been reported. In addition to the use of masks,[24] the selective deposition of parylene on micropatterned substrates featuring variable surface chemistries has been reported as a viable approach to microstructure CVD-based coatings.[25−27] In these studies, the CVD deposition of commercially available parylene,[26] as well as of functionalized nanofilms,[27] was inhibited by the presence of metals.

The motivation of this study was to create nanosheet membranes using a versatile fabrication procedure that consists in (i) selective deposition of functional poly-*p*-xylylenes on micropatterned substrates and (ii) the subsequent removal of the nanomembranes from the substrate to create free-standing nanosheets. The CVD polymerization of functional [2.2]paracyclophanes is the critical step in this approach as (i) it leads to the fabrication of a wide range of different chemically functionalized polymer coatings, (ii) the controlled thickness of the CVD coating can be as low as a few nanometers, and finally (iii) solventless microstructuring techniques have already been integrated into the CVD polymerization process, providing control over the membrane geometry. Herein, we report on the direct fabrication of microstructured functional polymer nanofilms by selective chemical vapor deposition polymerization on micropatterned self-assembled monolayers (SAMs). This one-step coating process is used for the production of ultrathin reactive polymer films, which can subsequently be etched from the substrate to obtain free-standing polymeric nanomembranes.

RESULTS AND DISCUSSION

Chemical Vapor Deposition Polymerization on Homogeneous SAM Substrates. Polymer nanofilms were fabricated by chemical vapor deposition (CVD) polymerization of functional [2.2]paracyclophane on SAM substrates. This vapor phase deposition process consists in the sublimation of a functional precursor under reduced pressure, followed by its pyrolysis, leading to reactive dimers that spontaneously polymerize on a cold substrate, thus forming a functional nanofilm. Preliminary CVD polymerizations have been performed on homogeneous SAMs. For this purpose, SAMs have been grown by immersing gold substrates in ethanolic solutions of 11-mercapto-1-undecanol (MUD), 16-mercaptohexadecanoic acid (MHDA), or 1-hexadecanethiol (HDT). Then, 4-trifluoroacetyl [2.2]paracyclophane and 4,15-dichloro[2.2]paracyclophane were pyrolyzed at 660 °C under a reduced pressure (0.15 mbar), and the respective functional poly-*p*-xylylenes were deposited on the SAM-coated gold substrates, maintained at a temperature of 15 °C. Using a quartz crystal microbalance located in the deposition chamber, the approximate thickness of the polymer coating was monitored *in situ*. Two distinct deposition runs have been carried out to fabricate polymer coatings with different targeted thicknesses. As evidenced by the ellipsometry measurements shown in Table 1, poly(4-trifluoroacetyl-*p*-xylylene-*co*-*p*-xylylene) and poly(4-chloro-*p*-xylylene) were successfully coated on carboxyl- and hydroxyl-terminated SAMs (MHDA and MUD, respectively), whereas little deposition occurred on alkane-terminated SAMs (HDT). A thickness difference of around 13 nm was observed when poly(4-chloro-*p*-xylylene) was coated on MHDA or MUD compared to HDT. In the same way, poly(4-trifluoroacetyl-*p*-xylylene-*co*-*p*-xylylene) was around 5 nm thicker on MHDA or MUD than on HDT. Similar tendencies were observed when ultrathin nanofilms of 2 nm were fabricated.

Fabrication of Microstructured Polymer Nanofilms. To confirm the preferential deposition of functional poly-*p*-xylylene previously observed on carboxyl- and hydroxyl-terminated SAMs compared to alkane-terminated SAMs, CVD polymerization, targeting the fabrication of nanofilms of a few nanometers, was performed on micropatterned SAM-coated substrates. Scheme 1 illustrates the experimental procedure followed to entail selective polymer deposition. Laterally patterned SAMs on gold substrates were produced by microcontact printing (μCP).[28] Experimentally, a polydimethylsiloxane (PDMS) stamp with an array of squares of 3 μm × 3 μm was inked with an ethanolic solution of a first thiol molecule. The pattern was transferred to the gold surface by bringing the stamp into contact with the substrate. The area surrounding the patterned part was then filled with a second SAM by simple immersion of the patterned substrate in an ethanolic solution of the second thiol molecule. In this way, a regular pattern with 3 μm wide zones of MHDA/HDT (isolated MHDA-covered areas surrounded with HDT) and HDT/MUD (isolated HDT-covered areas surrounded with MUD) was produced.

CVD polymerization of 4-trifluoroacetyl[2.2]-paracyclophane and 4,15-dichloro[2.2]paracyclophane was subsequently performed on the micropatterned SAM substrates, as previously described on homogeneously coated SAMs. The topography of the coated samples was analyzed by atomic force microscopy (AFM). As noticeable in Figure 1, AFM micrographs confirm the preferential deposition observed by ellipsometry.

Functional parylene nanofilms were preferentially coated onto COOH- and OH-terminated SAMs compared to CH_3-terminated SAMs, according to thickness profiles. No mechanistic evidence has been obtained yet, but we hypothesis that such behavior originates from the polarity of the functional groups present on the SAMs that favors the interaction with functional *p*-xylylene reactive intermediates. Chemisorption of

TABLE 1. Thickness of the Functional CVD Polymer Layers, Poly(4-trifluoroacetyl-*p*-xylylene-*co*-*p*-xylylene) and Poly(4-chloro-*p*-xylylene), Measured by Ellipsometry, after Two Independent CVD Polymerizations onto Different Homogeneous SAMs

CVD coating	SAM	CVD thickness (nm)	
		Deposition 1 (2 nm targeted)	Deposition 2 (15 nm targeted)
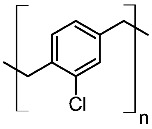	MHDA	2.2	18.5
	MUD	1.7	18.6
	HDT	0.5	5.7
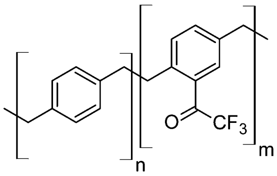	MHDA	2.2	13.9
	MUD	1.6	12.0
	HDT	1.1	8.2

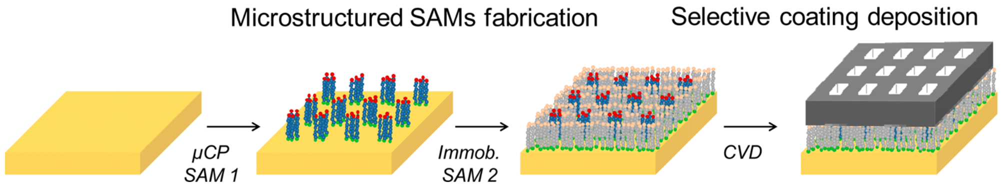

Scheme 1. Schematic representation of the selective deposition of a functional CVD coating onto microstructured SAMs. The first step corresponds to microcontact printing of SAM 1, the second step stands for the immobilization of SAM 2 backfilling the squared islands. and third step consists in the fabrication of a structured nanofilm by CVD polymerization.

these compounds may be more efficient on COOH- and OH-terminated SAMs than on CH_3-terminated SAMs, thus encouraging nucleation and propagation of the polymer chain growth. *Via* this preferential CVD deposition, MHDA/HDT samples led to the formation of functional poly-*p*-xylylene dots, located on top of MHDA squares. More interestingly, HDT/MUD samples enable the production of poly(4-trifluoroacetyl-*p*-xylylene-*co*-*p*-xylylene) on the surrounding area of the squares, where MUD was located. The poly(4-trifluoroacetyl-*p*-xylylene-*co*-*p*-xylylene) coating thus corresponds to a duplicate of the MUD location on the SAM-coated gold substrate. Since MUD forms a microstructured continuous phase on the SAM-coated sample, the deposition of the functional polymer on this sample also forms a microstructured continuous phase (polymer film as a duplicate of the functional SAMs). *Via* this combination of SAMs patterning of HDT/MUD on a gold substrate and the subsequent CVD polymerization of 4-trifluoroacetyl[2.2]paracyclophane, a continuous nanofilm of functional poly-*p*-xylylene, microstructured with 3 × 3 μm holes, was produced.

The preferential deposition of poly(4-trifluoroacetyl-*p*-xylylene-*co*-*p*-xylylene) on MUD was unambiguously confirmed by time-of flight secondary ion mass spectrometry (ToF-SIMS) measurements. Both secondary ion imaging and depth profiling by Cs^+ (500 eV) bombardment were performed on patterned poly(4-trifluoroacetyl-*p*-xylylene-*co*-*p*-xylylene) samples. Since the pattern was easily visible in the SIMS images, both areas grown on MUD and on HDT zones were separated and individual depth profiles reconstructed. Figure 2a shows the Au^- intensities in the depth profiles. Note that the plotted signal intensities have not been normalized for different areas on the sample, and Au_2^- signals follow the same trend. The depth profiles clearly show that gold appears closer to the surface in HDT regions than in MUD regions, originating from the presence of a thicker polymer layer deposited on MUD regions. Additionally, Figure 2b confirms the presence of CF_3 groups, whose content is mapped, in regions originally functionalized with MUD. These ToF-SIMS analyses undoubtedly confirmed the preferential deposition of poly(4-trifluoroacetyl-*p*-xylylene-*co*-*p*-xylylene) on MUD regions. If the deposition of the CVD polymer is sufficiently low and well-controlled, it is reasonable to expect the fabrication of ultrathin (few nanometers thick) microstructured nanosheets of functional poly-*p*-xylylenes.

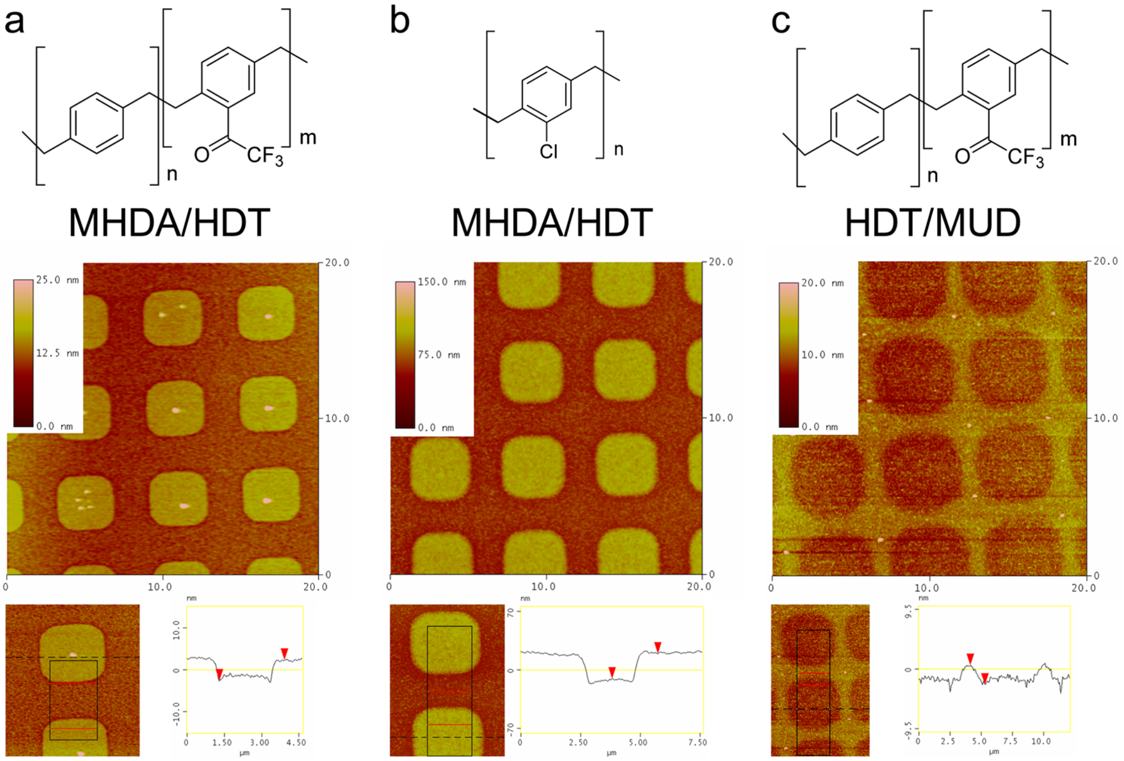

Figure 1. AFM images and profiles of poly(4-trifluoroacetyl-*p*-xylylene-*co*-*p*-xylylene) (a, c) or poly(4-chloro-*p*-xylylene) (b) films coated on patterned SAMs made of MHDA/HDT (a, b) and HDT/MUD (c).

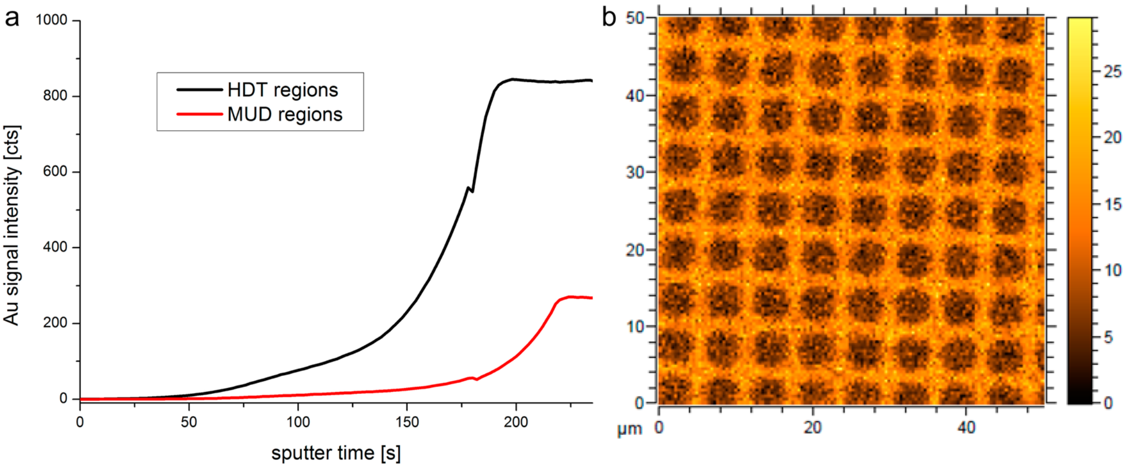

Figure 2. Poly(4-trifluoroacetyl-*p*-xylylene-*co*-*p*-xylylene) coated on patterned SAMs made of HDT/MUD: (a) Au content with respect to sputter time in HDT regions (black) and MUD regions (red); (b) ToF-SIMS images of the distribution of CF_3 groups (color scale corresponds to number of counts).

The production of 2 nm thick nanofilms of poly(4-trifluoroacetyl-*p*-xylylene-*co*-*p*-xylylene) on micropatterned HDT/MUD substrates was confirmed by monitoring the thickness profile of the sample by AFM (Figure 3c). The height profile of the substrate (Figure 3b, top curve) is in accordance with the expected thickness of the polymer nanofilm. A small amount of poly(4-trifluoroacetyl-*p*-xylylene-*co*-*p*-xylylene) islands might be present as well on HDT areas (Figure 3a), but, as described below, these islands do not lead to a cohesive polymer film on these areas that has sufficient mechanical integrity to be maintained if the film is removed from the substrate.

Nanofilm Removal for the Generation of a Free-Standing Nanomembrane. The most challenging issue was the handling of such ultrathin microstructured nanofilms and particularly the removal from the substrate. To obtain a free-standing structured nanosheet, an etching process of the gold substrate was carried out that was adapted from a procedure described in the literature.[30] The coated sample was immersed for 30 min in an aqueous solution of ferricyanide etchant

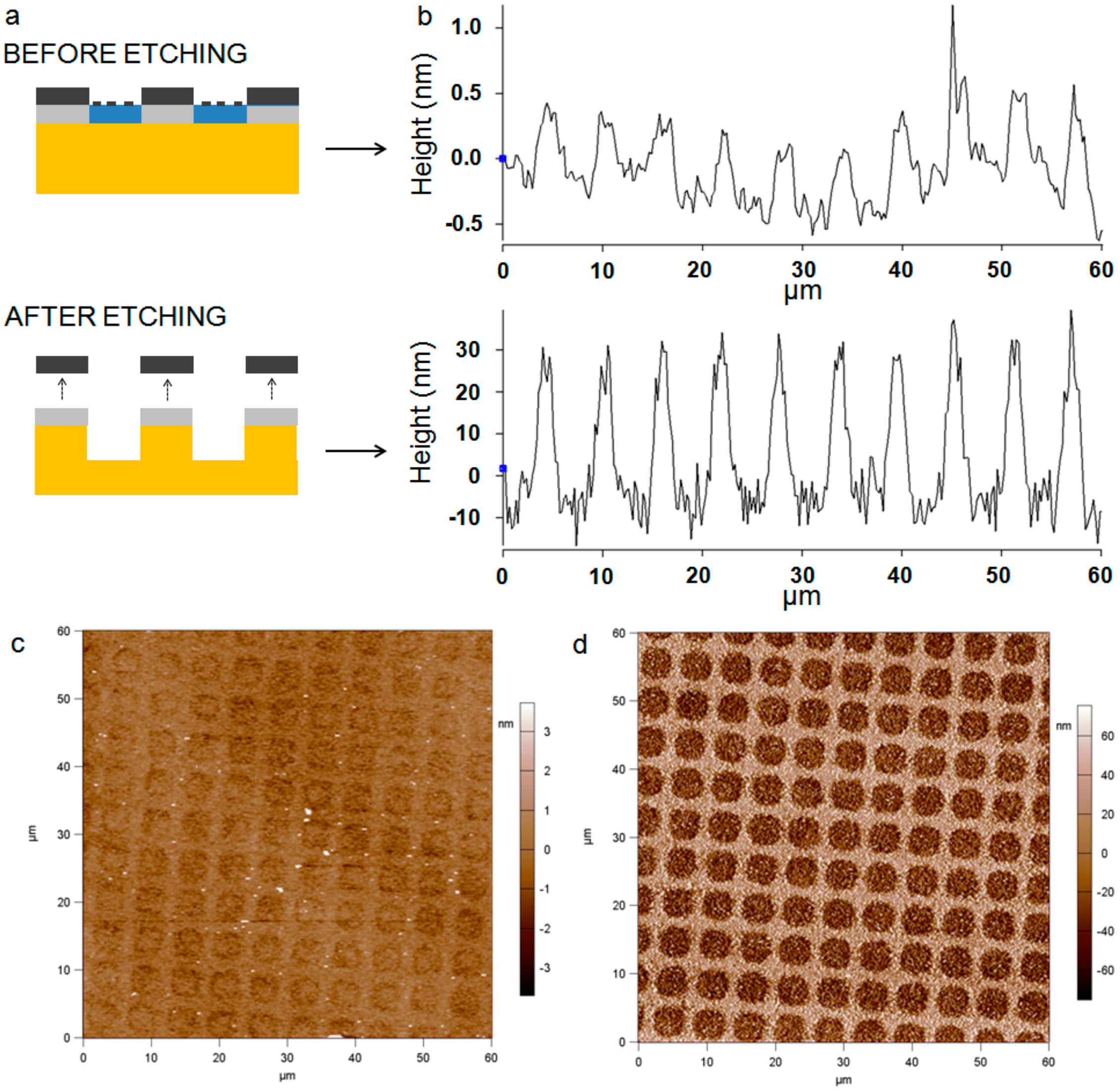

Figure 3. Etching process performed on a substrate coated with poly(4-trifluoroacetyl-*p*-xylylene-*co*-*p*-xylylene) on patterned SAMs made of HDT/MUD. (a) Schematic representation of the substrate before and after etching (yellow areas represent gold, light gray areas stand for MUD, blue areas are HDT, and dark gray areas represent the polymer film; the vertical and horizontal scales are independent). (b) Height profile of the substrate, measured by AFM before (top) and after (bottom) etching, and the corresponding AFM micrographs of the substrate (60 μm × 60 μm) (c) before and (d) after etching.

to aid the nanofilm removal from the surface. An AFM image of the substrate has been made before (Figure 3b upper profile and c) and after (Figure 3b lower profile and d) the etching process to investigate the efficiency of the procedure. After the etching procedure, the height profile confirms the presence of microfeatures (Figure 3b, lower curve), having approximately the same lateral size as those generated by microcontact printing (squares of 3 × 3 μm) and seen on the polymer coating before the etching procedure (Figure 3b upper profile). However, the height difference between the squares and the surrounding area is about 40 nm after etching, which is much higher than the thickness of the polymer coating (about 1–2 nm). The squares, previously not covered by the CVD nanofilm, appear as holes of 40 nm depth. This observation is in good agreement with the effect expected by the etching procedure, namely, the decrease of the gold layer thickness on the substrate, where no protective layer (polymer coating) was located. The diffusion of the etchant solution is faster, if no cohesive polymer film covers the surface. Therefore, the upper gold layer of the substrate, on which HDT was immobilized, was more rapidly etched than those below the polymer coating. The etching procedure continued until the polymer film spontaneously left the substrate when the upper nanometers of the gold layer were completely etched from the substrate.

Finally, a free-standing nanofilm was removed from the aqueous etchant solution *via* the use of a TEM grid, which later served as a support for the film as it was imaged by SEM, as shown in Figure 4. An ultrathin gold–palladium layer (3 nm thick) has been coated on the substrate to allow the visualization of the film.

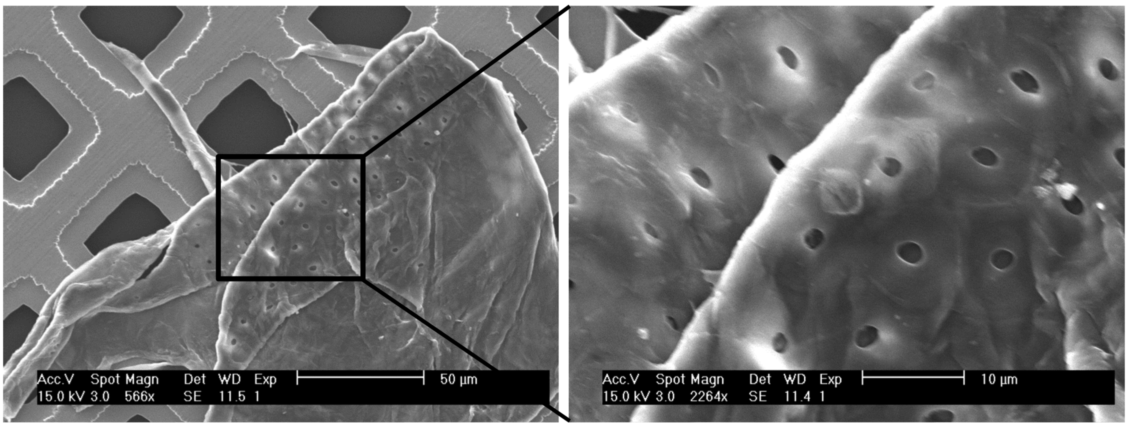

Figure 4. Poly(4-trifluoroacetyl-*p*-xylylene-*co*-*p*-xylylene) nanomembrane (1 to 2 nm thick), produced on patterned SAMs made of HDT/MUD, after its removal from the substrate. The film is pictured on a TEM grid.

The polymer film appears as a free-standing membrane. Holes of around 3 × 3 μm are clearly observable in the nanosheet and are regularly spaced. The holes do not appear on the entire nanosheet, as noticeable on the lower magnification micrograph, since this part of the nanofilm likely corresponds to the side of the micropatterned area (outside the patterned area, a continuous polymer film is fabricated, as this unpatterned area originates from the deposition of poly(4-trifluoroacetyl-*p*-xylylene-*co*-*p*-xylylene) on a homogeneous MUD region).

CONCLUSION

In summary, we have developed a novel fabrication process for functionalized nanomembranes featuring a thickness of only a few nanometers. This process is based on the selective deposition of a functional polymer by chemical vapor deposition polymerization on micropatterned self-assembled monolayers. To the best of our knowledge, it is the first time that the production of an ultrathin membrane of functional parylene has been reported. The presence of a microstructured nanofilm of poly(4-trifluoroacetyl-*p*-xylylene-*co*-*p*-xylylene) on patterned SAMs made of HDT/MUD has been evidenced by AFM and ToF-SIMS characterization, for which a clear mapping of CF_3 groups was achieved. Additionally, a film removal procedure has been developed to obtain free-standing microstructured polymer nanosheets. For this purpose, the etching of the SAM-coated gold substrate on which the polymer film was deposited has been performed with an aqueous ferricyanide solution, and the polymer nanosheet was fished out of the solution *via* a TEM grid, which then served as the support for the nanosheet as depicted by SEM micrographs. Selective CVD polymerization on SAMs is an elegant approach for the fabrication process of microstructured polymer nanofilms since the functional polymer is directly deposited on the micropatterned SAMs and since no metallic top layer is required during the deposition. The polymer nanofilm is produced in a one-step process and does not require additional cross-linking or film treatment to ensure its cohesion. Additionally, nanofilm production by CVD polymerization is a vapor phase process, which occurs at room temperature, enables a fine-tuning of film thickness, and is already developed for the production of various functional polymers. Therefore, this study paves the way for the fabrication of free-standing microstructured nanosheets made of functional polymers in order to develop ultrathin nanomembranes.

METHODS

Self-Assembled Monolayer Growth. Gold substrates were prepared by thermal vapor deposition (Silz, Germany) of 100 nm gold (99.995%, Chempur) onto polished silicon wafers (Wacker) precovered with a 5 nm titanium adhesion layer. Prior to SAM growth, the substrates were rinsed with absolute ethanol (Merck) and dried with nitrogen. Homogeneous (unpatterned) SAMs were deposited on gold substrates by simple immersion of the wafer in an ethanolic solution of 11-mercapto-1-undecanol (1 mM in absolute ethanol, Aldrich) for 1 day, 1-hexadecanethiol (1 mM in absolute ethanol, Aldrich) for 1 day as well, or 16-mercaptohexadecanoic acid (20 μM in a mixture containing 90 vol % ethanol and 10 vol % acetic acid, Aldrich) for 3 days. To fabricate laterally patterned SAMs on gold substrates, a microcontact printing method was used.[28] For instance a polydimethylsiloxane stamp with an array of squares of 3 μm × 3 μm was inked with a 1 mM ethanolic solution of HDT and dried with nitrogen.[29] The pattern was transferred to the gold surface by bringing the stamp into contact with the surface of the substrate for 2 min. The area surrounding the HDT patterned part was then filled with MUD SAM by simple immersion of the patterned substrate in a 1 mM MUD ethanolic solution. In this way, a regular pattern with 3 μm wide zones of hydroxyl-terminated SAM (MUD) between 3 μm large squares of alkane-terminated SAM (HDT) is produced. These micropatterned SAMs are named HDT/MUD. MHDA/HDT is prepared in a similar way, except that a 1 mM MHDA solution contains a mixture of

90 vol % ethanol and 10 vol % acetic acid and that the inked stamp was kept in contact with the substrate for 1 min.

Functional Parylene Nanofilm Deposition. Functional parylene nanofilms were subsequently deposited on microstructured SAM samples, as well as on gold references. For this purpose, CVD polymerization of two functional [2.2]paracyclophanes was performed in a custom-built CVD setup. 4-Trifluoroacetyl-[2.2]paracyclophane[31] was synthesized as described elsewhere, and 4,15-dichloro[2.2]paracyclophane was commercially available. The dimer precursor was sublimated under a reduced pressure (0.15 mbar) at a temperature close to 100 °C. Then, it entered the pyrolysis furnace, heated at 660 °C, with the help of an argon flow (20 sccm). Quinodimethane intermediates were formed and spontaneously polymerized on the substrate, maintained at 15 °C on the sample holder, located in the deposition chamber. A slow deposition rate (close to 0.2 Å/s), monitored by a quartz crystal microbalance located in the deposition chamber, is targeted to fabricate thin parylene nanofilms.

Removal of the Microstructured Nanofilm from the Substrate. Microstructured nanofilms deposited on patterned HDT/MUD were removed from the gold substrate by immersion of the samples in an aqueous solution containing 3.2 mg of potassium hexacyanoferrate(II) trihydrate ($K_4[Fe(CN)_6]$, $3H_2O$, Aldrich), 33 mg of potassium hexacyanoferrate(III) ($K_3[Fe(CN)_6]$, Aldrich), 210 mg of sodium thiosulfate ($Na_2S_2O_3$, Aldrich), and 800 mg of potassium hydroxide (Aldrich) in 10 mL of deionized water. In this way,[30] the gold was slowly etched, favoring the removal of the polymer film after 30 min. For subsequent analyses, the polymer film was fished from the aqueous solution with a TEM grid as support and the remaining substrate was washed with deionized water.

Conflict of Interest: The authors declare no competing financial interest.

Acknowledgment. The authors would like to thank P. Krolla-Siedenstein for optical microscopy images, as well as C. Hussal, D. Kratzer, and S. Goetz for technical support. They also acknowledge support from the BioInterfaces Program and the Nano Micro Facility at KIT. A.M.R. would like to acknowledge the Whitaker International Scholars Program for financial support.

Supporting Information Available: Experimental section: nanofilm characterization. Optical micrograph of the patterned PDMS stamp used to generate microstructured SAM substrates (Figure S1). Pseudo-3D image based on SIM depth profiling (Figure S2). This material is available free of charge *via* the Internet at http://pubs.acs.org.

REFERENCES AND NOTES

1. Cheng, W.; Campolongo, M. J.; Tan, S. J.; Luo, D. Free-standing Ultrathin Nano-membranes *via* Self-Assembly. *Nano Today* **2009**, *4*, 482–493.
2. Govindaraju, T.; Avinash, M. B. Two-Dimensional Nanoarchitectonics: Organic and Hybrid Materials. *Nanoscale* **2012**, *4*, 6102–6117.
3. Dreyer, D. R.; Ruoff, R. S.; Bielawski, C. W. From Conception to Realization: An Historial Account of Graphene and Some Perspectives for Its Future. *Angew. Chem., Int. Ed.* **2010**, *49*, 9336–9344.
4. Guo, S.; Dong, S. Graphene Nanosheet: Synthesis, Molecular Engineering, Thin Film, Hybrids, and Energy and Analytical Applications. *Chem. Soc. Rev.* **2011**, *40*, 2644–2672.
5. Jiang, C.; Markutsya, S.; Tsukruk, V. V. Compliant, Robust, and Truly Nanoscale Free-Standing Multilayer Films Fabricated Using Spin-Assisted Layer-by-Layer Assembly. *Adv. Mater.* **2004**, *16*, 157–161.
6. Vendamme, R.; Onoue, S. Y.; Nakao, A.; Kunitake, T. Robust Free-Standing Nanomembranes of Organic/Inorganic Interpenetrating Networks. *Nat. Mater.* **2006**, *5*, 494–501.
7. Eck, W.; Küller, A.; Grunze, M.; Völkel, B.; Gölzhäuser, A. Freestanding Nanosheets from Crosslinked Biphenyl Self-Assembled Monolayers. *Adv. Mater.* **2005**, *17*, 2583–2587.
8. Angelova, P.; Vieker, H.; Weber, N.-E.; Matei, D.; Reimer, O.; Meier, I.; Kurasch, S.; Biskupek, J.; Lorbach, D.; Wunderlich, K.; *et al.* A Universal Scheme to Convert Aromatic Molecular Monolayers into Functional Carbon Nanomembranes. *ACS Nano* **2013**, *7*, 6489–6497.
9. Decher, G. Fuzzy Nanoassemblies: Toward Layered Polymeric Multicomposites. *Science* **1997**, *277*, 1232–1237.
10. Mamedov, A. A.; Kotov, N. A. Free-Standing Layer-by-Layer Assembled Films of Magnetite Nanoparticles. *Langmuir* **2000**, *16*, 5530–5533.
11. Tang, Z. Y.; Kotov, N. A.; Magonov, S.; Ozturk, B. Nanostructured Artificial Nacre. *Nat. Mater.* **2003**, *2*, 413–418.
12. Nardin, C.; Winterhalter, M.; Meier, W. Giant Free-Standing ABA Triblock Copolymer Membranes. *Langmuir* **2000**, *16*, 7708–7712.
13. Goedel, W. A.; Heger, R. Elastomeric Suspended Membranes Generated *via* Langmuir−Blodgett Transfer. *Langmuir* **1998**, *14*, 3470–3474.
14. Fujie, T.; Okamura, Y.; Takeoka, S. Ubiquitous Transference of a Free-Standing Polysaccharide Nanosheet with the Development of a Nano-Adhesive Plaster. *Adv. Mater.* **2007**, *19*, 3549–3553.
15. Okamura, Y.; Kabata, K.; Kinoshita, M.; Saitoh, D.; Takeoka, S. Free-Standing Biodegradable Poly(lactic acid) Nanosheet for Sealing Operations in Surgery. *Adv. Mater.* **2009**, *21*, 4388–4392.
16. Coclite, A. M.; Howden, R. M.; Borrelli, D. C.; Petruczok, C. D.; Yang, R.; Yagüe, J. L.; Ugur, A.; Chen, N.; Lee, S.; Jo, W. J.; *et al.* 25th Anniversary Article: CVD Polymers: a New Paradigm for Surface Modification and Device Fabrication. *Adv. Mater.* **2013**, *25*, 5392–5423.
17. Sreenivasan, R.; Gleason, K. K. Overview of Strategies for the CVD of Organic Films and Functional Polymer Layers. *Chem. Vap. Deposition* **2009**, *15*, 77–90.
18. Gorham, W. F. A New, General Synthetic Method for the Preparation of Linear Poly-*p*-xylylenes. *J. Polym. Sci., Part A: Polym. Chem.* **1966**, *4*, 3027–3039.
19. Chen, H.-Y.; Lahann, J. Designable Biointerfaces Using Vapor-Based Reactive Polymers. *Langmuir* **2011**, *27*, 34–48.
20. Bally, F.; Cheng, K.; Nandivada, H.; Deng, X.; Ross, A. M.; Panades, A.; Lahann, J. Co-Immobilization of Biomolecules on Ultrathin Reactive Chemical Vapor Deposition Coatings Using Multiple Click Chemistry Strategies. *ACS Appl. Mater. Interfaces* **2013**, *5*, 9262–9268.
21. Lahann, J.; Balcells, M.; Rodon, T.; Lee, J.; Choi, I. S.; Jensen, K. F.; Langer, R. Reactive Polymer Coatings: A Platform for Patterning Proteins and Mammalian Cells onto a Broad Range of Materials. *Langmuir* **2002**, *18*, 3632–3638.
22. Suh, K. Y.; Langer, R.; Lahann, J. A Novel Photodefinable Reactive Polymer Coating and Its Use for Microfabrication of Hydrogel Elements. *Adv. Mater.* **2004**, *16*, 1401–1405.
23. Chen, H.-Y.; Hirtz, M.; Deng, X.; Laue, T.; Fuchs, H.; Lahann, J. Substrate-Independent Dip-Pen Nanolithography Based on Reactive Coatings. *J. Am. Chem. Soc.* **2010**, *132*, 18023–18025.
24. Chen, H.-Y.; Lahann, J. Vapor-Assisted Micropatterning in Replica Structures: A Solventless Approach towards Topologically and Chemically Designable Surfaces. *Adv. Mater.* **2007**, *19*, 3801–3808.
25. Vaeth, K. M.; Jackman, R. J.; Black, A. J.; Whitesides, G. M.; Jensen, K. F. Use of Microcontact Printing for Generating Selectively Grown Films of Poly(*p*-phenylene vinylene) and Parylenes Prepared by Chemical Vapor Deposition. *Langmuir* **2000**, *16*, 8495–8500.
26. Vaeth, K. M.; Jensen, K. F. Transition Metals for Selective Chemical Vapor Deposition of Parylene-Based Polymers. *Chem. Mater.* **2000**, *12*, 1305–1313.
27. Chen, H.-Y.; Lai, J. H.; Jiang, X.; Lahann, J. Substrate-Selective Chemical Vapor Deposition of Reactive Polymer Coatings. *Adv. Mater.* **2008**, *20*, 3474–3480.
28. Xia, Y. N.; Whitesides, G. M. Soft Lithography. *Angew. Chem., Int. Ed.* **1998**, *37*, 551–575.
29. Kumar, A.; Biebuyck, H.; Whitesides, G. Patterning Self-Assembled Monolayers - Applications in Materials Science. *Langmuir* **1994**, *10*, 1498–1511.

30. Xia, Y. N.; Zhao, X. M.; Kim, E.; Whitesides, G. M. A Selective Etching Solution for Use with Patterned Self-Assembled Monolayers of Alkanethiolates on Gold. *Chem. Mater.* **1995**, *7*, 2332–2337.
31. Lahann, J.; Choi, I. S.; Lee, J.; Jensen, K. F.; Langer, R. A New Method toward Microengineered Surfaces Based on Reactive Coating. *Angew. Chem., Int. Ed.* **2001**, *40*, 3166–3169.